communications biology

A Nature Portfolio journal

Article

https://doi.org/10.1038/s42003-025-07820-7

Effector CD8 T cell differentiation in primary and breakthrough SARS-CoV-2 infection in mice

Brock Kingstad-Bakke[1], Woojong Lee[1], Boyd L. Yount Jr.[2], Thomas Cleven[1], Hongtae Park[1], Jeremy A. Sullivan[1], Ralph C. Baric[2] & M. Suresh[1]

The nature of the effector and memory T cell response in the lungs following acute SARS-CoV-2 infections remains largely unknown. To define the pulmonary T-cell response to COVID-19, we compared effector and memory T-cell responses to SARS-CoV-2 and influenza A virus (IAV) in mice. Both viruses elicited potent effector T cell responses in lungs, but memory T cells showed exaggerated contraction in SARS-CoV-2-infected mice. Specifically, unlike the T-bet/EOMES-driven effector transcription program in IAV lungs, SARS-CoV-2-specific CD8 T cells embarked on a STAT-3-centric transcriptional program, a defining characteristic of a pro-fibro-inflammatory program: limited cytotoxicity, diminished expression of tissue-protective inhibitory receptors (PD-1, LAG-3, and TIGIT), and augmented mucosal imprinting (CD103). Circulating CD45RO^{+}HLA-DR^{+} CD8 T cells in hospitalized COVID-19 patients expressed elevated levels of STAT-3 and low levels of TIGIT. IL-6 blockade experiments implicated IL-6 in STAT-3 induction and downregulation of PD-1 expression on SARS-CoV-2-specific primary effector CD8 T cells. Memory CD8 T cells specific to a single epitope, induced by mucosal vaccination, differentiated into cytotoxic effectors and expressed high levels of CD103, effectively reducing viral burden in lungs following a breakthrough SARS-CoV-2 infection. Our findings have implications for developing targeted immunotherapies to mitigate immunopathology and promote protective T cell immunity to SARS-CoV-2.

As of 2024, SARS-CoV-2 has resulted in almost 800 million infections globally, with more than 6 million deaths, and the virus has continued to evolve with over 12,000 distinct strains identified to date[1,2]. It is very clear that newer variants, such as Omicron and its sub-lineages, exhibit significant resistance to neutralization by antibodies generated from previous infections or vaccinations, necessitating updated vaccine formulations and booster doses to enhance protection[3,4].

Recent studies have highlighted the critical role of CD8 T cells in controlling not just primary infections, but also preventing re-infections and reducing disease severity in breakthrough cases[5]. However, phenotypic and functional profiles of circulating T cells in COVID-19 patients with severe disease suggest a spectrum of T-cell dysregulation ranging from severe depletion to senescence, exhaustion, aberrant Th17 differentiation, and hyperactivation[6–9]. It is unclear whether the spectrum of T-cell abnormalities in COVID-19 patients represents different stages of the disease or is influenced by the host's prior immunity and genetic factors[10]. Further, findings of dysregulated T-cell immunity in severely ill patients are confounded by ongoing anti-viral and anti-inflammatory therapies. Analysis of SARS-CoV-2 CD8 T cells during the acute phase of infection showed that cells had high proliferative potential, displayed lower expression of terminal differentiation markers, low expression of inhibitory molecules, and subsets of spike-specific CD8 T cells had a lower than expected proportion of cells expressing effector function and cytotoxic T lymphocyte (CTL) molecules[11,12]. It is also noteworthy that most of the information to date on human T-cell responses to SARS-CoV-2 is derived from analysis of circulating T cells, and the nature of pulmonary T-cell immunity, especially the differentiation and/or persistence of effector and memory T cells remains underexplored.

We previously demonstrated that vaccination of mice with adjuvanted spike protein via mucosal or parenteral routes conferred protection against lethal SARS-CoV-2[13]. Additionally, we demonstrated that spike-expressing mRNA vaccines elicited robust spike-specific CD8 T cells that trafficked from the circulation to the airways, providing protection against viral challenge[14]. However, the nature of the primary CD8 T cell response in the

[1]Department of Pathobiological Sciences, University of Wisconsin-Madison, Madison, WI, USA. [2]Department of Microbiology and Immunology, University of North Carolina-Chapel Hill, Chapel Hill, NC, USA. e-mail: sureshm@vetmed.wisc.edu

lungs following SARS-CoV-2 infection, and the subsequent differentiation of these effector T cells into memory T cells, and the impact of SARS-CoV-2 infection on character of the recall CD8 T cell responses of vaccine-elicited memory CD8 T cells in the absence of cross-reactive CD4 T cells or neutralizing antibody responses, remains unknown.

In this study, we compared the pulmonary T cell responses between an acute resolving SARS-CoV-2 infection and a well-characterized acute influenza A virus (IAV) infection in mice. We specifically investigated the differentiation of effector and memory T cells in these different acute viral infections. These studies provided fundamental insights into altered transcriptional programming of CD8 T cell effector functions, mucosal imprinting and expression of inhibitory molecules in lungs of SARS-CoV-2-infected mice. In addition to our investigation of primary effector and memory T cell responses to SARS-CoV-2 and IAV in K18-hACE2 and WT C57BL/6 mice, we extended our study to evaluate whether: (1) breakthrough SARS-CoV-2 infections also dysregulate recall effector CD8 T cell responses of vaccine-induced memory CD8 T cells in the lungs; (2) parenteral or intranasal vaccine-induced memory CD8 T cells specific to a single epitope, can protect against breakthrough SARS-CoV-2 infection in the apparent absence of recall CD4, antibodies and B cell responses. Data presented in this manuscript have provided fundamental insights into the potential role of immunological milieu in driving disparate programs of effector differentiation during acute infections with SARS-CoV-2 and IAV. Further, findings from the current study reinforces the importance of lung-resident memory CD8 T cells in protection against SARS-CoV-2, especially when CD8 T cell reactivity of recall responses is restricted to a single epitope. These findings have implications in understanding pulmonary immunity to acute viral infections and the development of T-cell-based vaccines to protect against viral infections of the respiratory tract.

Results

Antigen-specific CD8 T-cell responses to SARS-CoV-2 and influenza A virus (IAV) in the respiratory tract of K18-hACE2 transgenic mice

Here we compared CD8 T-cell responses to the USA-WA1/2020 strain of SARS-CoV-2 (100 PFU) and PR8/H1N1 strain of IAV (50 PFU), by infecting K18-hACE2tg mice with pre-determined viral doses that led to similar kinetics of viral control in lungs (Fig. 1A). At day 8 and 10 post-infection (PI), we quantified SARS-CoV-2-specific (K^b/S525 epitope) and IAV-specific (D^b/NP366 epitope) CD8 T-cell responses in lungs (Fig. 1B) using MHC I tetramers. Remarkably high frequencies and numbers of virus-specific CD8 T cells were detected in lungs of SARS-CoV-2- and IAV-infected mice and these frequencies increased between days 8 and 10 PI. The frequencies of CD8 T-cell responses to these specific epitopes were comparable between the two infections.

Accelerated expression of CD103 and limited terminal differentiation of lung effector CD8 T cells in SARS-CoV-2 infection of K18-hACE2 transgenic mice

Under the influence of antigen receptor signaling and local inflammatory milieu (exposure to cytokines such as TGFβ, IL-10 and IL-15), effector CD8 T cells differentiate into lung/airway T_{RM}s that express varying levels of CD49a, CD69 and CD103[15,16]. Induction of these molecules is termed mucosal imprinting, and it was of interest to determine whether lung environment in SARS-CoV-2-infected mice affected mucosal imprinting of effector CD8 T cells. As shown in Fig. 1C, the percentages of $CD69^+$, $CD49a^+$ and $CXCR3^+$ CD8 T cells were comparable between SARS-CoV-2 and IAV lungs, on days 8 and 10 PI. However, effector CD8 T cells specific to NP366 in IAV lungs showed minimal expression of CD103 at day 8 and 10 PI, but SARS-CoV-2 lungs fostered CD103 expression in ~40% of S525-specific effector CD8 T cells between days 8 and 10 PI (Fig. 1C), indicating accelerated induction of mucosal imprinting marker CD103 in SARS-CoV-2 infection. Since effector CD8 T cells that express low levels of the senescence marker KLRG-1 are more likely to differentiate into T_{RM}s[16], we quantified expressions of KLRG-1 and CX3CR1 that are associated with terminal differentiation of effector CD8 T cells. Between days 8 and 10 PI, effector CD8 T cells in IAV lungs increased expressions of CX3CR1 and/or KLRG-1 (Fig. 1D). Remarkably, only a very small percentage of effector CD8 T cells in SARS-CoV-2 lungs expressed KLRG-1 or CX3CR1 at days 8 and 10 PI. While CD127 (IL-7 receptor) expression on CD8 T cells did not differ significantly between SARS-CoV-2 and IAV lungs at day 10 PI (Fig. 1D), the higher expressions of KLRG-1 and CX3CR1 in IAV lungs suggest greater terminal differentiation of effector CD8 T cells, as compared to those in SARS-CoV-2 lungs. In summary, SARS-CoV-2 lungs promoted CD103 expression and limited terminal differentiation of effector CD8 T cells, as compared to lungs of IAV-infected mice.

Impaired induction of lung-protective inhibitory (exhaustion) molecules on SARS-CoV-2-specific CD8 T cells in K18-hACE2 transgenic mice

During the resolution phase of an acute influenza virus infection, expressions of inhibitory molecules (also referred to as exhaustion markers) such as PD-1, TIM-3, TIGIT and LAG-3 on effector CD8 T cells limit the pro-fibrotic inflammatory response in lungs[17–19]. Since COVID-19 disease in humans is associated with a pro-fibro-inflammatory response in lungs[20,21], we determined whether expression of inhibitory molecules on effector CD8 T cells are dysregulated in lungs of SARS-CoV-2-infected mice. More than 40% of IAV-specific effector CD8 T cells expressed PD-1 and/or TIGIT and/or LAG-3 on days 8 and 10 PI (Fig. 2A and Supplementary Fig. 1A). In SARS-CoV-2 lungs however, on day 8 PI, only 25% of effector CD8 T cells expressed one of the three inhibitory molecules and this percentage dropped to 5% on day 10 PI (Supplementary Fig. 1A). Next, we determined whether reduced expression of inhibitory molecules was linked to defective induction of the master transcription factor TOX, which promotes the expression of PD-1, TIGIT and LAG-3[22]. Although the mean fluorescence intensities (MFIs) did not reflect this difference, a small yet significantly higher percentage ($P < 0.05$) of effector CD8 T cells expressed transcription fcator TOX in IAV lungs compared to those in SARS-CoV-2 lungs at day 10 PI (Supplementary Figs. 1B and 2) Supplementary Fig. 2. Tempered expression of inhibitory molecules was also associated with increased percentages of $Ki67^+$ SARS-CoV-2-specific proliferating CD8 T cells in lungs, in comparison to IAV-specific CD8 T cells (Supplementary Fig. 1B). Thus, the immunological elements that induce TOX and inhibitory molecules to mitigate a potentially pro-fibrotic inflammatory response in lungs of IAV-infected mice might be diminished in SARS-CoV-2 lungs.

SARS-CoV-2 and IAV elicit disparate signaling and effector transcription programs in lung CD8 T cells of K18-hACE2 transgenic mice

Next, we probed whether the aforementioned differences in cell surface phenotypes of effector CD8 T cells in SARS-CoV-2 and IAV lungs were associated with alterations in the expression of granzyme B and transcription factors T-bet, EOMES, IRF-4, RORγt, GATA-3 and STAT-3[23,24] that regulate effector differentiation. At day 8 and 10 PI, 90–100% of NP366-specific effector CD8 T cells in IAV lungs expressed high levels of granzyme B, while only 65–75% of S525-specific effector CD8 T cells expressed granzyme B in SARS-CoV-2 lungs (Fig. 2B). Strikingly, at both days 8 and 10 PI, the percentages of $IRF\text{-}4^+$/granzyme B^+ effector CD8 T cells in SARS-CoV-2 lungs were significantly lower ($P < 0.05$) than in the lungs of IAV-infected mice (Fig. 2B and Supplementary Fig. 2). Notably, the expression levels of CD107a, a marker for degranulation, were comparable between effector CD8 T cells in SARS-CoV-2 and IAV lungs (Fig. 2B). This suggests that while granzyme B expression differed between the two groups, the capacity for degranulation was not significantly altered.

While EOMES levels were significantly lower in SARS-CoV-2 lung CD8 T cells than in IAV lungs (Fig. 2C, Supplementary Fig. 2), no significant differences ($P < 0.05$) were observed in the expression of T-bet, BATF, RORγt and Bcl-2 between SARS-CoV-2- and IAV-specific CD8 T cells (Fig. 2C, Supplementary Fig. 1C). A significantly ($P < 0.05$) greater percentage of effector CD8 T cells in SARS-CoV-2 lungs expressed elevated

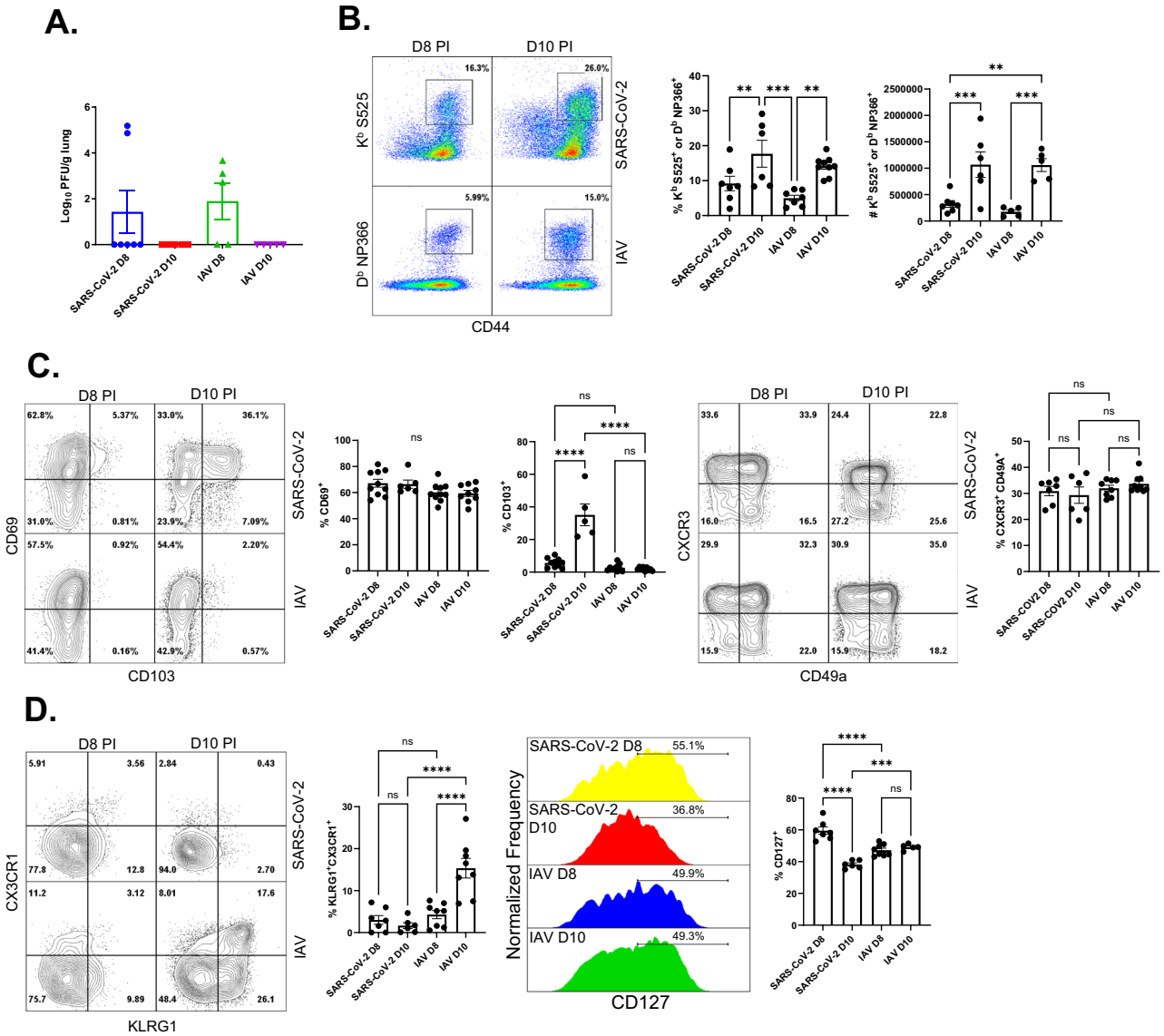

Fig. 1 | Primary effector T-cell responses to SARS-CoV-2 and Influenza Virus in K18-ACE2 transgenic mice. K18-ACE2tg mice were intranasally infected with 50 PFU of the PR8/H1N1 strain of influenza A virus or 100 PFU of the USA-WA1/2020 (WA strain) of SARS-CoV-2. **A** Following influenza or SARS-CoV-2 infection, virus titers were measured in lungs. Single-cell suspensions of lungs were stained with viability dye, followed by K^b/S525 (for SARS-CoV-2) or D^b/NP366 tetramers (for IAV) in combination with anti-CD4, CD8, CD44, CD69, CD103, CD49a, CX3CR1, KLRG1, CD127, CXCR3. **B** Frequencies of NP366- or S525-specific CD8 T cells in the lung among gated CD8 T cells. **C**, **D** FACS plots or histograms are gated on K^b/S525 or D^b/NP366 tetramer-binding CD8 T cells. The numbers are percentages of $CD103^+$, $CXCR3^+$/$CD49a^+$, $KLRG1^+$/$CX3CR1^+$, $CD127^+$ cells in respective gates or quadrants. Data represent four independent experiments. Data in each graph indicate mean ± SEM.

levels of both total STAT-3 and phosphorylated STAT-3 (p-STAT3), as compared to their expression levels in IAV-specific effector CD8 T cells (Fig. 2D, Supplementary Fig. 2, and Supplementary Fig. 3). To assess whether STAT-3 upregulation is epitope-specific, we compared STAT-3 levels between S525- and N219-specific effector CD8 T cells at day 8 after infection. STAT-3 levels were not significantly different ($p = 0.84$) between S525 (MFI; 249.8 ± 87.87)- and N219 (MFI; 225.0 ± 75.6)-specific CD8 T cells. Since STAT-3 is known to oppose the cytotoxic effector program in CD8 T cells[25,26], these data suggested that SARS-CoV-2 infection might limit the CD8 T-cell-mediated cytotoxicity, including granzyme B expression by inducing STAT-3. Activated $CD44^{HI}$ CD4 T cells in lungs of SARS-CoV-2 mice also expressed significantly higher levels of STAT3 and GATA-3, than in CD4 T cells from lungs of IAV mice (Supplementary Fig. 4B). These data supported the inference that the immunological milieu in lungs of SARS-CoV-2 but not IAV mice might support a mixed T1/T2 functional programming. The observed alterations in the differentiation of SARS-CoV-2-specific CD8 T cells was not associated with changes in the percentages of $Foxp3^+$ regulatory CD4 T cells (Supplementary Fig. 4B).

In order to gain further insight into the signaling basis for altered expressions of CD103, inhibitory molecules and granzyme B during SARS-CoV-2 infection, we assessed phosphorylation states of STAT-5, AKT and ERK1/2 in effector CD8 T cells, in addition to STAT-3. Significantly ($P < 0.05$) greater percentages of IAV-specific effector CD8 T cells expressed p-AKT1 and p-ERK1/2, as compared to SARS-CoV-2-specific effector CD8 T cells (Supplementary Fig. 3B). These data are consistent with previously reported ongoing T cell receptor signaling in lungs of IAV mice[17], and such signaling appears to be substantively tempered in SARS-CoV-2-infected mice. The levels of both total STAT-3 and p-STAT-3, and p-STAT-5 appeared to be reciprocally regulated in effector CD8 T cells from lungs of SARS-CoV-2- and IAV-infected mice (Fig. 2, Supplementary Fig. 3A), with SARS-CoV-2 infection leading to elevated total and phosphorylated STAT-3 levels. Elevated levels of STAT-3 and p-STAT-3 (Fig. 2, Supplementary

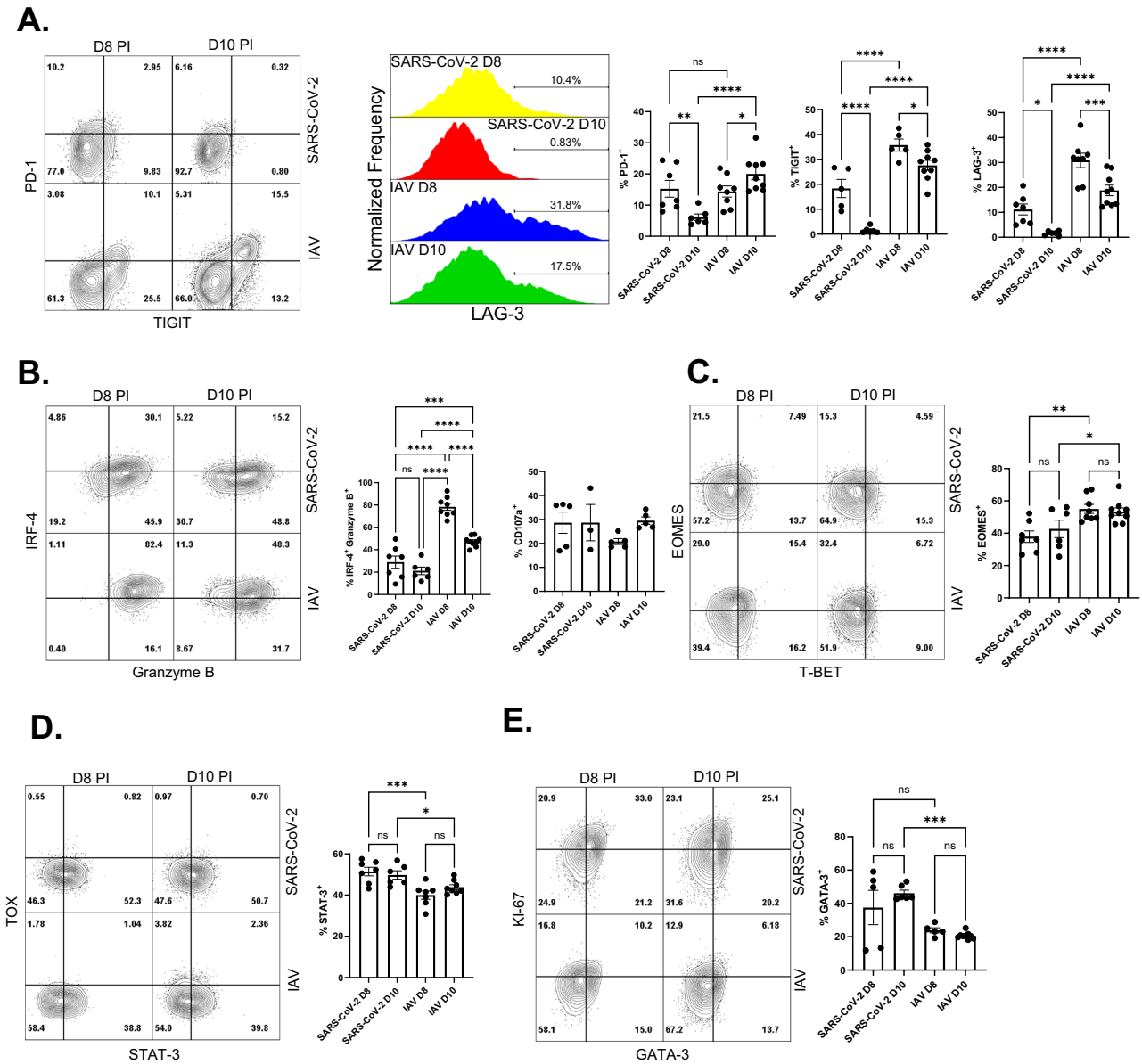

Fig. 2 | Aberrant transcriptional programming of effector T cells in lungs of SARS-CoV2-infected mice. K18-ACE2tg mice were intranasally infected with either IAV or the WA strain of SARS-CoV-2, and lung cells stained as described in Fig. 1. FACS plots in (**A**–**E**) are gated on tetramer-binding CD8 T cells, and data are the percentages of cells among the gated population for the indicated marker. Data represent four independent experiments. Data in each graph indicate mean ± SEM.

Fig. 3A) were defining characteristics of SARS-CoV-2-specific CD8 T cells, but the levels of p-STAT-5 were significantly greater ($P < 0.05$) in IAV-specific CD8 T cells, than in SARS-CoV-2-specific CD8 T cells (Supplementary Fig. 3A). These data strongly suggested that signaling inputs for effector CD8 T cells in SARS-CoV-2 lungs and IAV lungs are likely distinct.

Phosphorylated STAT-3 in SARS-CoV-2 lung CD8 T cells might reflect exposure to high levels of IL-6, a feature of severe COVID-19[27,28], and anti-IL-6 therapy improves recovery from severe COVID-19 in humans[29–34]. To determine whether STAT-3 induction and downregulation of granzyme B or inhibitory molecules in effector CD8 T cells are downstream to IL-6 signaling, we treated cohorts of SARS-CoV-2-infected K18-ACE2tg mice with anti-IL-6 or isotype control antibodies. At day 8 after infection, anti-IL-6 treatment did not affect the accumulation of SARS-CoV-2-specific effector CD8 T cells in lungs (Supplementary Fig. 5A). However, IL-6 blockade resulted in a statistically significant ($P < 0.05$): (1) reduction in percentages of STAT-3^{HI} CD8 T cells (Supplementary Fig. 5B); and (2) increase in the percentages of PD-1^{HI} CD8 T cells (Supplementary Fig. 5B), in comparison to those in the isotype control group. No significant alteration in expressions of granzyme B or LAG-3 in CD8 T cells occurred in response to anti-IL-6 treatment of SARS-CoV-2-infected mice (Supplementary Fig. 5B). Thus, CD8 T-cell responses to SARS-CoV-2 were largely unaffected by IL-6 blockade, which suggested that STAT-3 induction and altered differentiation of effector CD8 T cells might be driven in part by IL-6.

Because STAT-3 and GATA-3 are drivers of T2 and/or T17 differentiation[24], we examined antigen-triggered cytokine production by SARS-CoV-2- and IAV-specific CD8 and CD4 T cells, ex vivo (Fig. 3, Supplementary Fig. 6A). Upon ex vivo antigenic stimulation, SARS-CoV-2- and IAV-specific CD8 and CD4 T cells produced IFN-γ and the percentages of IFN-γ-producing CD8 T cells increased between day 8 and 10 PI only in SARS-CoV-2 lungs. Approximately 75% of cytokine-producing CD8 T cells produced IFN-γ alone or in combination with IL-2 and/or TNFα, (Fig. 3, Supplementary Fig. 6B), suggesting that both infections skewed CD8 T cells to a Tc1 polarity. Interestingly, at both days 8 and 10, the proportion of IFN-γ^{+} CD8 T cells that also produced TNFα and IL-2 (triple cytokine-producers)

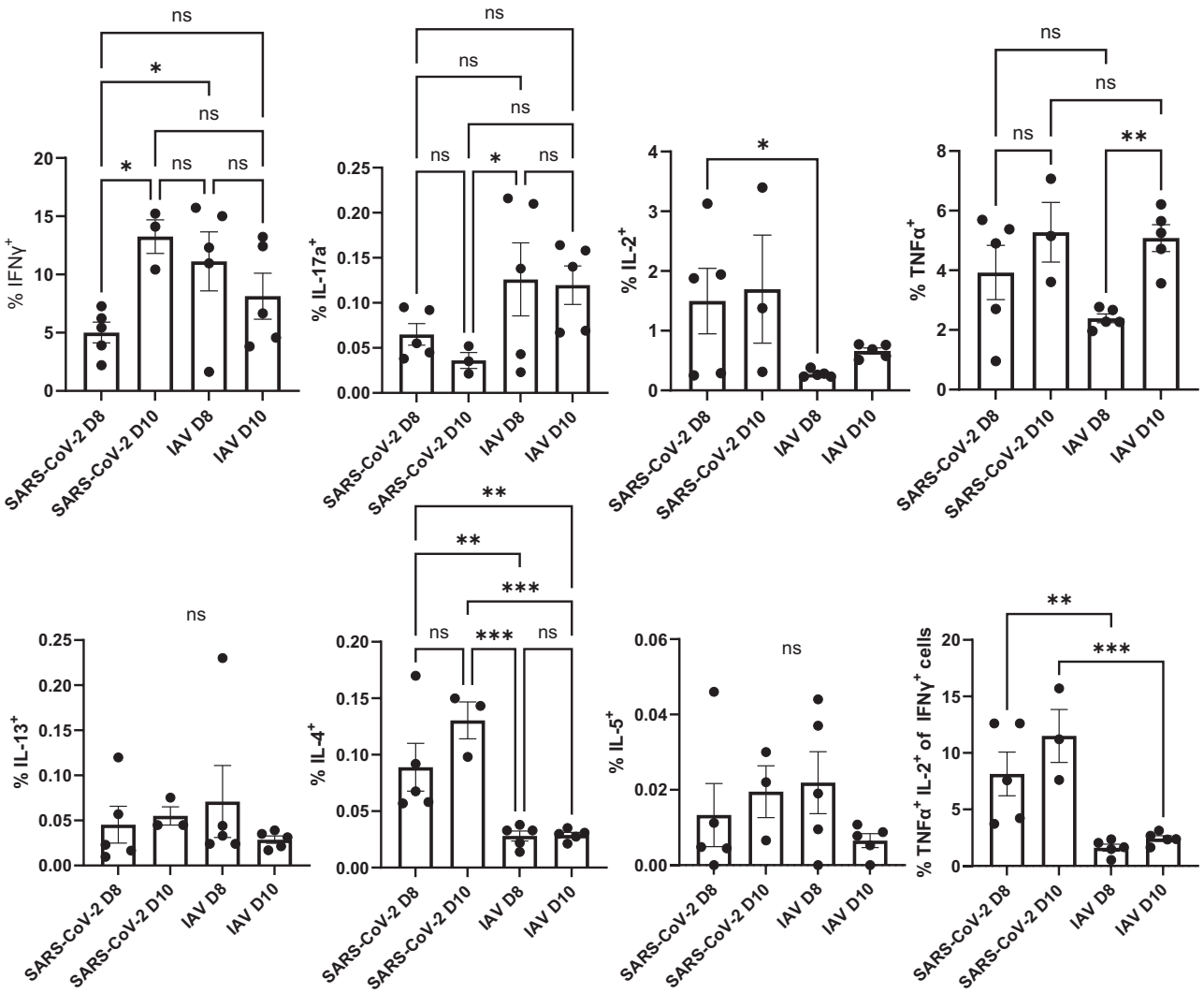

Fig. 3 | Functional programming of effector CD8 T cells in lungs of SARS-CoV-2 and influenza virus-infected mice. K18-ACE2tg mice were intranasally infected with either IAV or WU strain of SARS-CoV-2 viruses, and lung cells stained as described in Fig. 1. Lung cells from infected mice were stimulated with the S525 peptide of SARS-CoV-2 Spike (S) protein, or the NP366 peptide of IAV Nucleoprotein (NP). Cytokine production by CD8 T cells was assessed by intracellular cytokine staining. Percentages of cytokine-producing cells among the gated CD8 T cells are shown. Data represent four independent experiments. Data in each graph indicate mean ± SEM.

was 7–8 fold higher in lungs of SARS-CoV-2 mice, as compared with CD8 T cells in lungs of IAV mice (Fig. 3, Supplementary Fig. 6B). In order to assess whether lung CD8 T cells were dysfunctional, we determined the ratio of frequencies of tetramer$^+$ cells to cytokine-producing cells (that produced at least one of the following cytokines: IFN-γ, TNF-α, IL-2, IL-4, IL-5, IL-13 or IL-17). As shown in **Supplemental Fig. D**, the ratios of tetramer$^+$: cytokine-producing CD8 T cells were close to 1, and there was no significant difference between infections for the frequencies of multi-cytokine expressing cells (cells that expressed two or more of the measured cytokines: IFN-γ, TNF-α, IL-2, IL-4, IL-5, IL-13 or IL-17), which suggested that virus-specific CD8 T cells in lungs were equivalently functional in both SARS-CoV-2- and IAV-infected mice.

CD4 T cells from SARS-CoV-2 lungs and IAV lungs were stimulated with a spike protein peptide pool or a specific epitope peptide (NP311) respectively, but the frequencies of IFN-γ-producing CD4 T cells in lungs of IAV-infected mice were ~2-fold greater than in SARS-CoV-2-infected mice (Supplementary Fig. 6A). Akin to CD8 T cells, the polyfunctionality of lung CD4 T cells differed between the two infections (Supplemental Fig. 6A, C). First, it is noteworthy that the proportion of CD4 T cells that exclusively expressed TNF-α in SARS-CoV-2 lungs (52–67%) were substantively higher than in IAV lungs (29–32%). Second, the proportion of TNF-α-producing CD4 T cells outnumber IFN-γ-producing CD4 T cells in lungs of SARS-CoV-2-infected but not IAV-infected mice. Third, the percentages of CD4 T cells that produced IFN-γ along with TNF-α and/or IL-2 in IAV lungs (27-43%), as well as polyfunctional expression of IFN-γ, TNF-α and IL-2 together was greater than in SARS-CoV-2 lungs (7-14%) (Supplementary Fig. 6A, C). A small percentage of CD8 T cells in SARS-CoV-2 lungs produced IL-4, but there were clearly detectable populations of CD4 T cells that produced IL-4 and/or IL-13 in SARS-CoV-2 lungs, as compared to those in IAV lungs (Supplementary Fig. 6A). Thus, elevated levels of STAT-3 and GATA-3 in lung CD4 T cells of SARS-CoV-2 mice might drive functional polarization of a small fraction of virus-specific CD4 T cells into T_H2 cells.

SARS-CoV-2 infection in humans increases STAT-3 expression in CD4 and CD8 T cells

To determine if aberrant T-cell effector programming observed in mouse studies translated to a clinical setting, we analyzed PBMCs from healthy volunteers and patients hospitalized with a confirmed severe SARS-CoV-2 infection. Overall percentages of CD45RO$^+$ cells were similar between

healthy and SARS-CoV-2-infected groups, but SARS-CoV-2 patients had higher frequencies of HLA-DR$^+$ CD8 and CD4 T cells than in healthy volunteers, suggestive of an ongoing response to infection (Supplementary Fig. 7A, D); a substantive proportion of HLA-DR$^+$ CD8 T cells in SARS-CoV-2 group was proliferating, as measured by elevated expression of Ki-67 (Supplementary Fig. 7A, D). Since there is contradicting information about the functionality of T cells in patients with COVID-19[35–40], we examined their expression in human PBMCs from our patient cohort. We found that PD-1, LAG-3, and TIM-3 levels were not significantly elevated in CD8 T cells from patients with severe COVID-19, as compared to healthy volunteers (Supplementary Fig. 7B). Additionally, TIGIT levels were significantly lower on CD8 T cells in SARS-CoV-2 patients than in healthy volunteers (Supplementary Fig. 7B). Similarly, levels of effector molecules granzyme B and perforin, as well as the terminal differentiation marker CX3CR1, were not elevated in CD8 T cells, despite patients being in the acute phase of SARS-CoV-2 infection (Supplementary Fig. 7C). These findings are suggestive of variability in CD8 T-cell responses among different patient populations. Of interest was that total STAT-3 levels were significantly higher in CD4 and CD8 T cells in SARS-CoV-2-infected patients, as compared to healthy volunteers (Supplementary Fig. 7C, E). Although we measured STAT-3 levels in human T cells, elevated STAT-3 expression has been associated with altered STAT-3 signaling activity and functional consequences in other studies[41,42] Notably however, in our study, circulating activated HLA-DR$^+$ CD8 T cells in COVID-19 patients displayed elevated levels of STAT-3 expression but did not show significant alterations in the expressions of effector molecules (granzyme B and perforin) or inhibitory molecules such as PD-1.

Characteristics of SIINFEKL-specific effector and memory CD8 T cells in lungs of C57BL/6 mice infected with mouse-adapted strains of SARS-CoV-2 and IAV

Data presented so far were derived from infection of K18-hACE2 transgenic mice infected with the Wuhan strain of SARS-CoV-2 or the prototypic IAV, focusing on responses to virus-specific epitopes. While the K18-hACE2 transgenic mice are highly susceptible to human strains of SARS-CoV-2 without adaptation, viral infection of the central nervous system and elevated severity of the infection are confounding factors associated with this animal model of SARS-CoV-2 infection. Additionally, in these studies, we did not rule out the epitope-specific effects on T cell differentiation by comparing T cells of the same antigenic specificity between SARS-CoV-2 and IAV. In order to address the afore-mentioned potential pitfalls, we infected C57BL/6 mice with mouse-adapted strains of SARS-CoV-2 (CoV-OVA) and PR8 strain of IAV that express the K^b-restricted ovalbumin SIINFEKL epitope (IAV-OVA). Importantly, this mouse-adapted SARS-CoV-2 strain faithfully recapitulates several features of human COVID-19 disease in immunocompetent non-transgenic mice and mitigate the caveats of the K18-ACE2 transgenic mice[43].

We infected groups of 10-week-old C57BL/6 mice with either 1000 PFU of CoV-OVA or 500 PFU of IAV-OVA; these doses induced comparable morbidities in infected mice. At 8- and 10-days post-infection (PI), both viruses elicited high frequencies of SIINFEKL-specific CD8 T cells in lungs, that peaked at day 10 after infection (Fig. 4A). At day 10 PI, the frequencies of SIINFEKL-specific CD8 T cells in IAV-OVA lungs were ~2-fold higher than in CoV-OVA lungs. Interestingly, the frequencies of S525-specific CD8 T cells were highest on day 8 after CoV-OVA infection and NP366-specific CD8 T cell frequencies peaked at day 10 after IAV-OVA infection. In summary, the overall antigen-specific CD8 T cell responses in the lungs of CoV-OVA and IAV-OVA mice were largely comparable.

Remarkably, data in Fig. 4B show that the distinguishing phenotypic characteristics of effector CD8 T cells in lungs of SARS-CoV-2 or IAV-infected K18-ACE2 transgenic mice (Fig. 1C, D) were fully recapitulated in SIINFEKL-specific effector CD8 T cells isolated from the lungs of CoV-OVA or IAV-OVA infected C57BL/6 mice. Specifically, SIINFEKL-specific effector CD8 T cells in CoV-OVA lungs displayed augmented levels of mucosal imprinting (elevated CD69$^+$ CD103$^+$ frequencies at day 10) and significantly lower degree of terminal differentiation (reduced frequencies of KLRG-1$^+$CX3CR1$^+$ cells and increased frequencies of CD127$^+$ cells at day 10), as compared to levels in IAV-OVA lungs; SIINFEKL-specific effector CD8 T cells in IAV-OVA lungs displayed greater degree of terminal differentiation (greater levels of KLRG-1$^+$CX3CR1$^+$ cells), than their counterparts in CoV-OVA lungs. Similar to our findings in lung CD8 T cells from IAV or SARS-CoV-2-infected K18ACE2 transgenic mice (Fig. 2A), a significantly greater percentages of SIINFEKL-specific effector CD8 T cells in lungs of IAV-OVA mice expressed the inhibitory molecules PD-1 and TIGIT, as compared to those in CoV-OVA lungs (Fig. 4B). Additionally, SIINFEKL-specific CD8 T cells from IAV-OVA-infected mice contained significantly higher levels of granzyme B and lower levels of STAT-3, whereas CD8 T cells from CoV-OVA-infected mice displayed significantly lower levels of granzyme B and higher levels of STAT-3 (Fig. 4C). Taken together, data in Figs. 2 and 4 provide strong evidence that SARS-CoV-2 infection might trigger a distinct STAT3-dominated program of effector CD8 T cell differentiation, which enforces diminished cytolytic effector function and potentially fosters pro-fibrotic immunopathology in the lungs.

Data in Figs. 1–4 demonstrated salient differences in effector T cell differentiation following infections with SARS-CoV-2 and IAV. Especially intriguing was the accelerated or augmented expression of the canonical tissue residency marker CD103, reduced terminal differentiation and the reduced expression of PD-1 on CD8 T cells in the lungs of SARS-CoV-2-infected mice. This is because, reduced terminal differentiation, PD-1 signaling and CD103 expression in effector CD8 T cells are known to promote development and/or persistence of lung-resident memory T cells[44]. It was of interest to assess whether differences in the expression of PD-1, CD103, and terminal differentiation altered the differentiation of tissue-resident memory CD8 T cells in the respiratory tract. We infected cohorts of C57BL/6 mice with CoV-OVA or IAV-OVA, and quantified SIINFEKL-specific memory CD8 T cells in airways (bronco-alveolar lavage; BAL), lungs, and spleen, at 60 days after infection. Frequencies and total numbers of SIINFEKL-specific CD8 T cells were significantly lower in the BAL, lung, and spleen of CoV-OVA-infected mice, compared to IAV-OVA-infected mice (Supplementary Fig. 8A). Furthermore, frequencies and numbers of S525-specific CD8 T cells were consistently lower in all tissues of CoV-OVA-infected mice compared to NP366-specific CD8 T cells in IAV-OVA-infected mice (Supplementary Fig. 8B).

To evaluate the tissue-resident memory (T_{RM}) phenotype of SIINFEKL-specific memory CD8 T cells at this time point, we assessed the co-expression of CD69 and CD103 in the BAL and lungs (Supplementary Fig. 8C). In the BAL, the frequencies of CD69$^+$/CD103$^+$ SIINFEKL-specific CD8 T cells ranged from 20% to 60%, with no significant differences observed between the CoV-OVA and IAV-OVA groups. However, in the lungs, the frequencies of CD69$^+$/CD103$^+$ SIINFEKL-specific CD8 T cells were significantly higher in IAV-OVA-infected mice, as compared to both doses of CoV-OVA-infected mice ($p < 0.05$). Similar trends were observed for S525- and NP366-specific CD8 T cells (Supplementary Fig. 8D), where IAV-infected mice exhibited higher frequencies of CD69$^+$/CD103$^+$ cells in the lungs compared to SARS-CoV-2-infected mice. These results indicate that despite the enhanced mucosal imprinting observed during the effector phase of SARS-CoV-2 infection, the establishment of lung T_{RM} cells at memory time points was less efficient, as compared to IAV infection.

Epitope-specific vaccination elicits robust CD8 T cell responses and reduces viral loads in SARS-CoV-2 challenge models

Data provided so far demonstrated that immunological milieu in the lungs might drive a distinct effector differentiation program during a primary T cell response (naïve to effector differentiation) to SARS-CoV-2 infection. What is unknown is whether SARS-CoV-2 infection dysregulates differentiation of effector CD8 T cells from vaccine-induce memory CD8 T cells during recall responses. Therefore, using two different vaccine strategies, we asked whether vaccine-induced memory CD8 T cells specific to a single epitope, can differentiate into effector cells and effectively reduce viral load in lungs, following challenge with SARS-CoV-2. The two vaccination

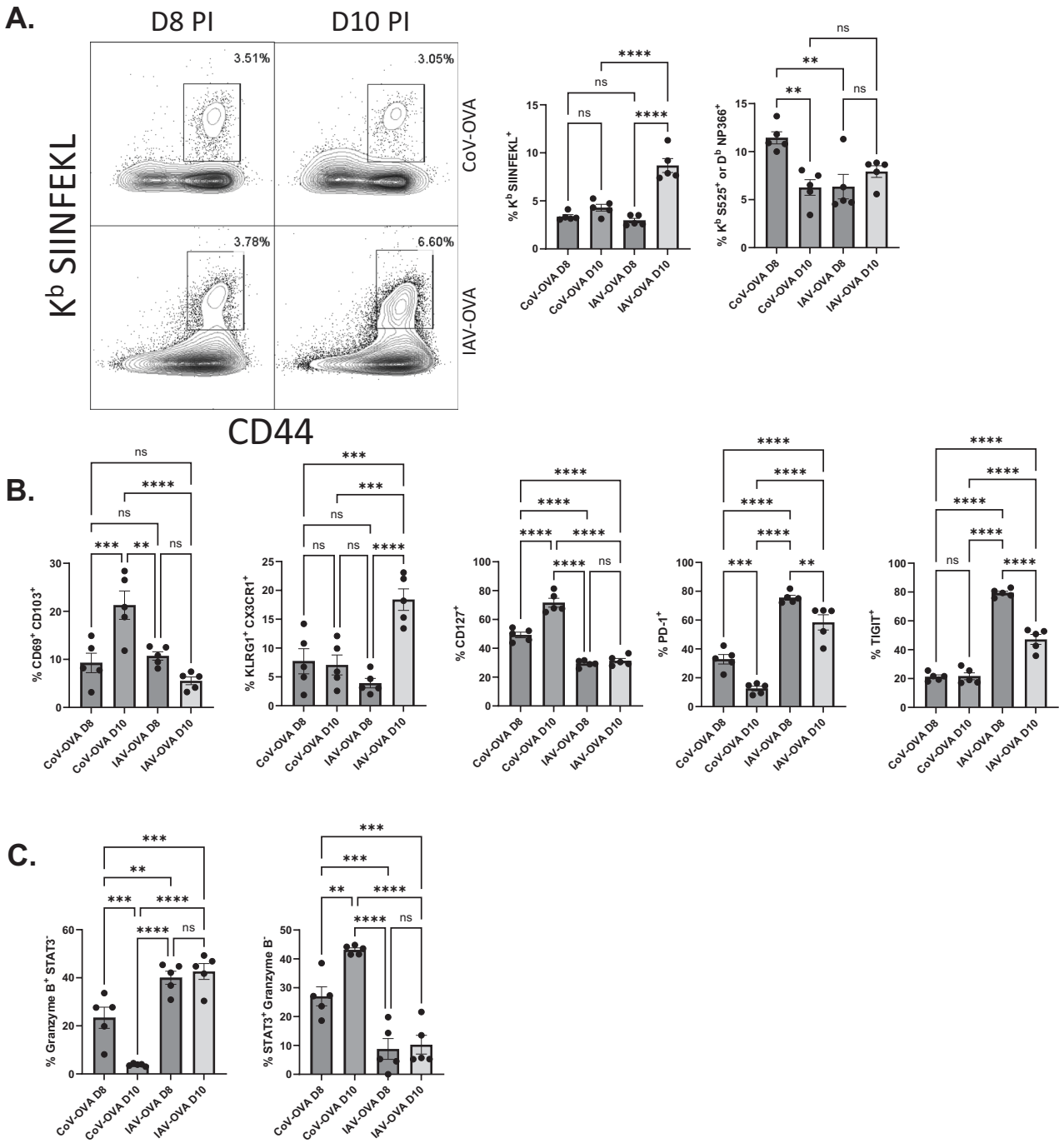

Fig. 4 | Comparative CD8 T cell responses in WT mice infected with CoV-OVA or IAV-OVA. WT C57BL/6 mice were infected with 1000 PFU of CoV-OVA or 500 PFU of IAV-OVA. On days 8 and 10 post-infection, mice were euthanized, and lungs were collected for CD8 T cell analysis. **A** FACS plots and graphs show frequencies of SIINFEKL-specific CD8 T cells in the lungs. **B** Graphs show frequencies of CD69 + CD103+, KLRG1 + CX3CR1+, CD127+, PD-1+, and TIGIT+ or **C** frequencies granzyme B+, and STAT-3+ among SIINFEKL-specific CD8 T cells. Data represent two independent experiments. Data in each graph indicate mean ± SEM.

models entail immunizing mice with chicken ovalbumin (formulated in an adjuvant) or infection with recombinant vaccinia virus expressing chicken ovalbumin (VV-OVA). Following vaccination, mice are challenged with CoV-OVA that expresses the K^b-restricted SIINFEKL epitope of OVA. It is noteworthy that viral control in this model is solely driven by SIINFEKL-specific memory CD8 T cells in the absence of antigenic stimulation of memory CD4 T cells or B cells.

Groups of mice were vaccinated intranasally or subcutaneously with OVA protein formulated in Adjuplex and CpG; this adjuvant combination was previously shown to confer durable protection to SARS-CoV-2[14]. For rigor, cohorts of mice were vaccinated with influenza NP protein via both routes as a negative control. On days -5, -3, -1, 1, and 3, relative to the lethal challenge with CoV-OVA, cohorts of vaccinated mice were treated with depleting anti-CD8 T cell antibodies (administered both intranasally and intravenously). On day 5 after challenge, mice were euthanized to assess viral loads and CD8 T cell responses in lungs. Flow cytometric analysis (Fig. 5) showed that mice vaccinated with ADJ+CpG plus OVA protein via the IN route displayed recall SIINFEKL-specific CD8 T cell response, with

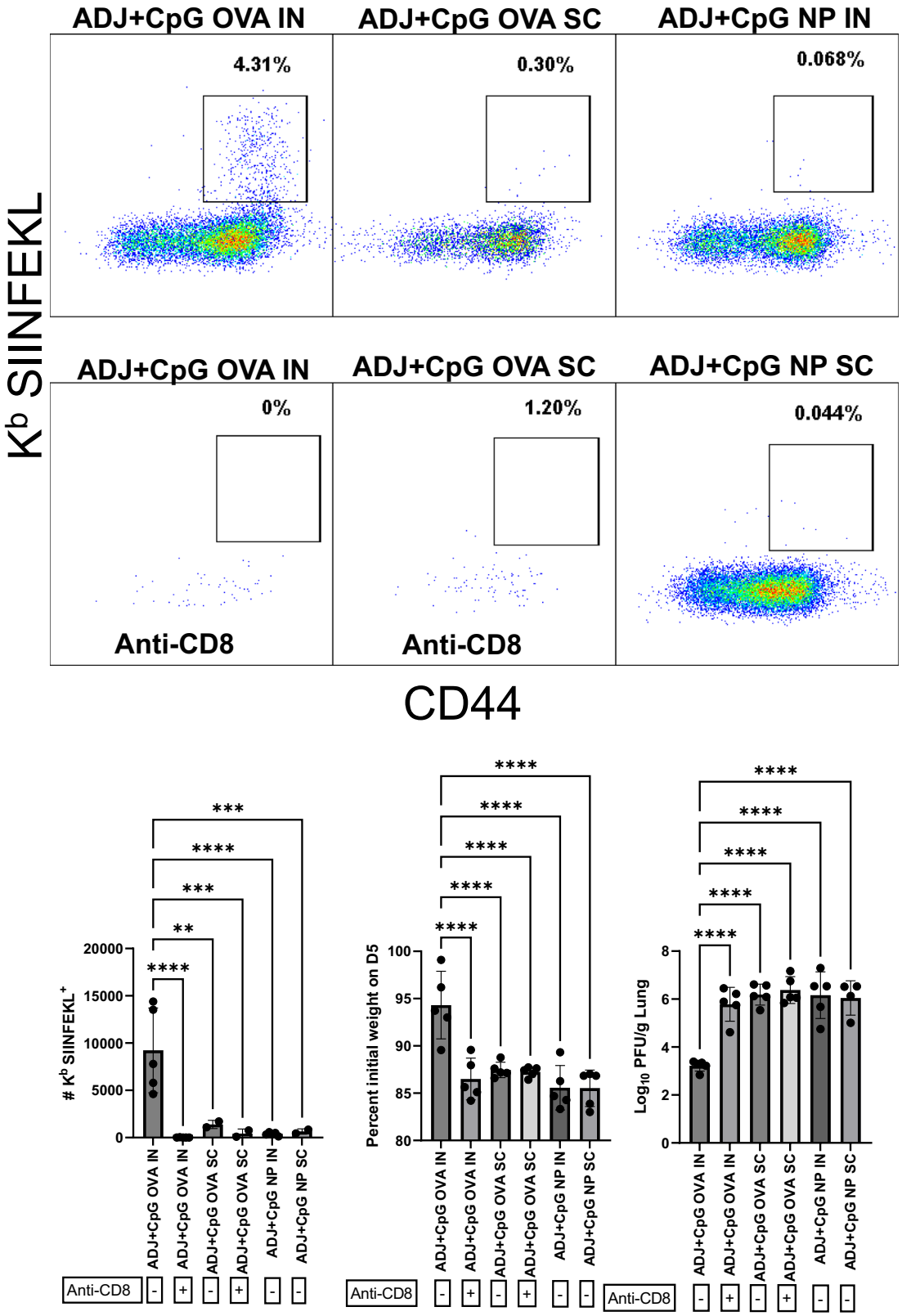

Fig. 5 | SIINFEKL-specific CD8 T cell responses following ADJ + CpG vaccination and CoV-OVA challenge. WT C57BL/6 mice were vaccinated with 5% Adjuplex plus 10 μg of CpG and 10 μg of OVA or NP protein via subcutaneous (SC) or intranasal (IN) routes, followed by challenge with CoV-OVA. Cohorts of mice were administered CD8 T cell depleting antibody by combined IV and IN routes. On day 5 post-challenge, lungs were collected for CD8 T cell and viral load analysis. Graphs show flow cytometric analysis of recall SIINFEKL-specific CD8 T cells, weight loss measurements, and quantification of lung viral loads. Data are representative of two experiments. Data in each graph indicate mean ± SEM.

significantly higher numbers of CD8 T cells in the lungs compared to all other groups. Notably, there was no significant difference in the numbers of SIINFEKL-specific CD8 T cells in the lungs of mice vaccinated subcutaneously with ADJ+CpG plus OVA compared to negative control NP protein-vaccinated mice, or OVA-vaccinated groups depleted of CD8 T cells. Importantly, mice in the IN ADJ+CpG plus OVA group exhibited significantly less weight loss, around only 5%, as compared to approximately 15% weight loss in all other groups at day 5 post-challenge. Additionally, there was a significant 3 $\log_{10}$ fold decrease in lung viral loads in the IN ADJ +CpG plus OVA group compared to all other groups. Thus, SIINFEKL-specific memory CD8 T cells induced by adjuvanted vaccine (administered intranasally) provided significant protection against weight loss, and effectively reduced SARS-CoV-2 load in lungs by >99% in a CD8 T cell-dependent fashion.

Using a complementary strategy, we vaccinated cohorts of mice with VV-OVA via intranasal (IN) or intramuscular (IM) routes. As a negative control, mice cohorts were vaccinated (IN or IM) with VV expressing the nucleoprotein (NP) of lymphocytic choriomeningitis virus (LCMV; VV-NP). Thirty-six days after vaccination, to mimic a breakthrough infection, mice were challenged with the CoV-OVA. Five days post-challenge, mice were euthanized to assess CD8 T cell recall responses and viral titers in lungs. Flow cytometric analysis (Fig. 6A) revealed that mice vaccinated with VV-OVA via the IN route exhibited significantly higher frequencies of SIINFEKL-specific CD8 T cells compared to those vaccinated via the IM route. Both VV-OVA vaccinated groups (IN and IM) demonstrated significantly higher frequencies of SIINFEKL-specific CD8 T cells than the negative control groups vaccinated with VV-NP. Furthermore, the VV-OVA IN group showed markedly lower viral titers in the lungs, as compared to all other groups, with a four-fold reduction relative to the negative control groups. Although the VV-OVA IM group also exhibited a significant reduction in viral titer, the decrease was only two-fold compared to the controls (Fig. 6B).

We also assessed whether SIINFEKL-specific effector CD8 T cells in lungs of SARS-CoV-2-challenged mice differentiated into effector cytotoxic lymphocytes. Flow cytometric analysis revealed that >60% of SIINFEKL-specific recall CD8 T cells expressed readily detectable levels of granzyme B in the lungs of SARS-CoV-2 challenged mice (Fig. 6C), suggestive of effector differentiation. By contrast, memory CD8 T cells specific to the VV B8R protein expressed little granzyme in the lungs of SARS-CoV-2-challenged mice because only SIINFEKL-specific memory CD8 T cells but not BR8-specific memory CD8 T cells are expected to respond to CoV-OVA challenge by differentiating into granzyme B-expressing effector CD8 T cells. These data suggested that recall of cytotoxic effector functions in memory CD8 T cells occurs effectively following challenge with SARS-CoV-2. Interestingly, unlike elevated granzyme B expression, expressions of KLRG-1 and CX3CR1 were comparable between SIINFEKL-specific and B8R-specific CD8 T cells (Fig. 6C). Next, we examined whether SARS-CoV-2 drove enhanced expression of CD103 in recall/secondary CD8 T cells, similar to lung effector CD8 T cells during a primary SARS-CoV-2 infection (Fig. 4B). While only a small fraction of quiescent B8R-specific memory CD8 T cells expressed CD103, nearly 80% of SIINFEKL-specific effector CD8 T cells expressed CD103 in lungs of SARS-CoV-2-challenged mice (Supplementary Fig. 9A). The expression of CD103 on recall lung CD8 T cells was likely induced by SARS-CoV-2 challenge because the frequencies of $CD103^+$ cells among SIINFEKL-specific memory CD8 T cells were lower in unchallenged mice, as compared to those in virally challenged mice (Supplementary Fig. 9B). Thus, SARS-CoV-2 infection drives enhanced expression of CD103 on both primary and recall effector CD8 T cells in lungs. Taken together, data in Fig. 4 suggested that unlike in a primary infection (Figs. 1–2), the immunological milieu induced by the breakthrough SARS-CoV-2 infection did not adversely affect the differentiation of vaccine-induced memory T cells into effectors, and their ability to reduce viral burden in lungs.

Discussion

A thorough characterization of antiviral T-cell immunity is a prerequisite for deciphering viral pathogenesis and developing effective, durable, and broadly protective vaccines against SARS-CoV-2. In this manuscript, we explored the nature and regulation of T-cell immunity during acute SARS-CoV-2 infection in the respiratory tract, comparing it to the well-characterized T-cell responses to an acute infection with the PR8/H1N1 strain of influenza A virus. This comparative analysis shows that the immunological environment and the range of signaling inputs orchestrated by influenza and COVID-19 in the lungs are distinct, driving different programs of effector differentiation in responding CD8 T cells. These differences influence processes such as trafficking, effector functions, mucosal imprinting, T_{RM} fate adaptation, and the regulation of inflammation or immunopathology. The findings presented in this manuscript provide new insights into the mechanisms governing the protective and pro-fibro-inflammatory roles of CD8 T cells in acute SARS-CoV-2 infection.

We find that infection with viral doses that caused comparable levels and duration of viral replication stimulated strong CD8 T-cell responses to defined epitopes of SARS-CoV-2 and IAV in the lungs of K18-ACE2tg mice. Interestingly, however, responding CD8 T cells in the lungs of SARS-CoV-2-infected mice exhibit significant differences in cell surface phenotype, function, and expression of transcription factors, as compared to those in IAV-infected mice. Effector CD8 T cells in lungs of SARS-CoV-2-infected mice display accelerated induction of CD103 and reduced expression levels of terminal differentiation markers KLRG-1 and CX3CR1. Although CD127 expression levels were similar between the two infections at day 10 PI, the higher expressions of KLRG-1 and CX3CR1 in IAV lungs indicate more terminal differentiation of effector CD8 T cells. These findings suggest that SARS-CoV-2 infection might promote accelerated mucosal imprinting but limit terminal differentiation of effector CD8 T cells in the lungs[16]. Our data in mice mimics enhanced T_{RM}-like cells in SARS-CoV-2-infected humans[9,45]. Among several factors, exposure of effector T cells to cytokines such as TGF-β might have promoted expression of CD103[15,16] because, high levels of TGF-β are induced in human COVID-19 patients[21]. An unexpected finding in this study was that, unlike IAV-specific effector CD8 T cells, SARS-CoV-2-specific CD8 T cells in lungs express low levels of inhibitory molecules PD-1, LAG-3 and TIGIT. This is a key finding because CD8 T-cell expression of inhibitory molecules protects lungs from immune-mediated fibrosis during the resolution phase of influenza virus infection[17–19]. Data on the expression of exhaustion-associated molecules in circulating CD8 T cells of human COVID-19 patients is equivocal[35–40]. In our human patient cohort, we did not observe significant elevation of PD-1 or LAG-3 markers. The contradicting findings on the expression of exhaustion markers is likely due to differences in patient demographics, disease severity, timing of sample collection, or technical variations. Nevertheless, our findings highlight the heterogeneity of immune responses in COVID-19 patients and suggest that factors such as the stage of infection and individual patient characteristics may influence the expression of these molecules. Despite these caveats, similar to our findings in mice, in one particular study, circulating CD8 T cells in human COVID-19 patients also expressed low levels of inhibitory molecules[46]. Therefore, pertaining to the reported fibro-inflammatory response in lungs of COVID-19 patients[47,48], we plan on investigating whether induction of pro-fibrotic cytokine TGF-β along with the dampened expression of inhibitory molecules on effector CD8 T cells promote lung fibrosis.

In comparison to IAV-specific effector CD8 T cells, a substantive fraction of SARS-CoV-2-specific effector CD8 T cells in lungs expressed lower levels of the effector molecule granzyme B and inhibitory molecules such as PD-1. Comparable expression of CD69 and similar kinetics of viral control in lungs between the two infections suggest that differences in TCR signaling might not explain muted expression of granzyme B or inhibitory molecules in SARS-CoV-2-specific CD8 T cells, but further investigations into viral antigen archiving in lungs and draining lymph nodes will be needed to address the underlying mechanisms[49,50]. A key finding from this study is that effector CD8 T cells in lungs of SARS-CoV-2-infected mice and circulating CD8 T cells in human COVID-19 patients contained elevated levels of the transcription factor STAT-3. In our mouse studies, we observed elevated levels of both total STAT-3 and phosphorylated STAT-3

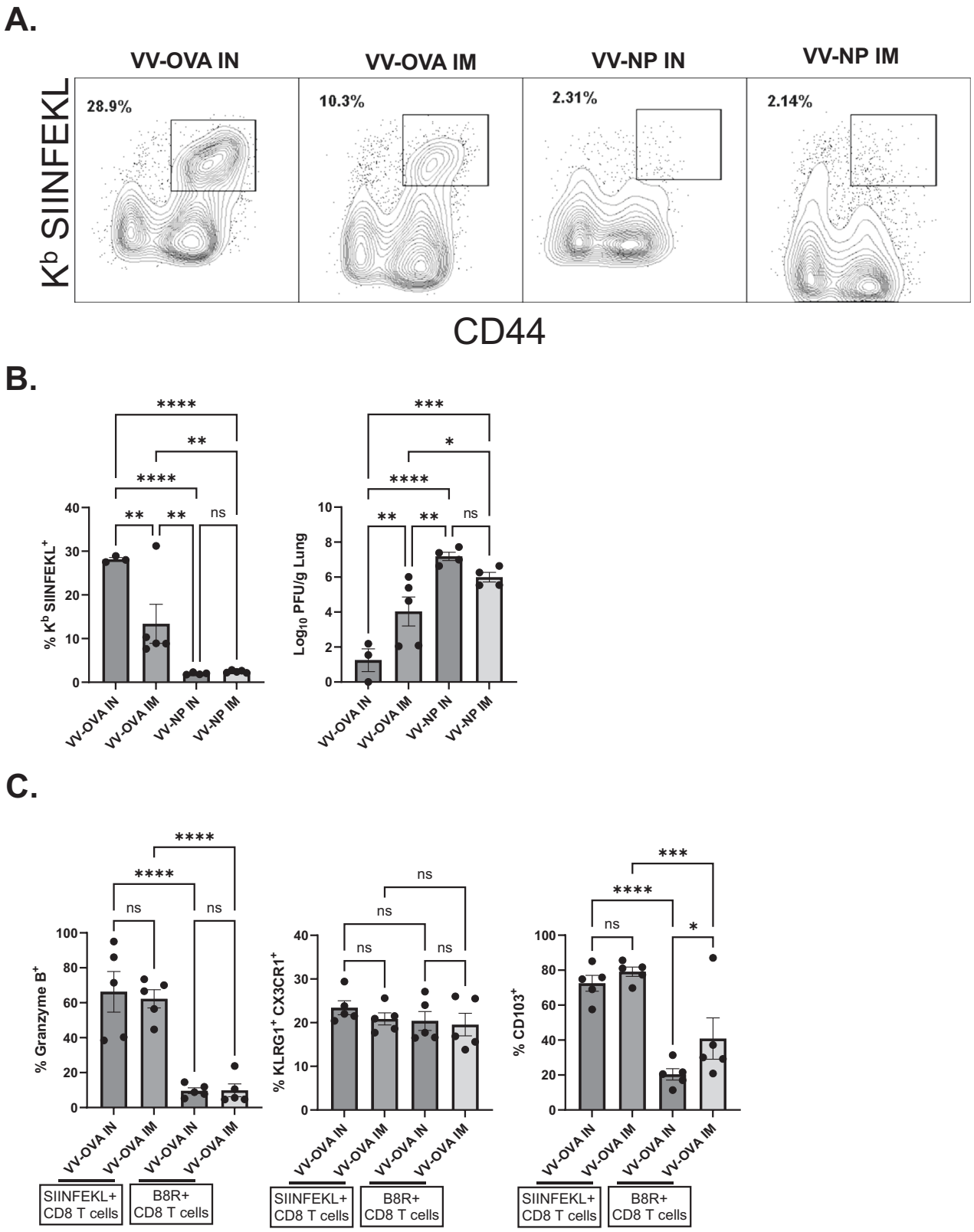

Fig. 6 | Recall responses and viral loads in mice vaccinated with replicating vaccinia virus expressing OVA. WT C57BL/6 mice were vaccinated with vaccinia virus (VV) expressing OVA or lymphocytic choriomeningitis virus (LCMV) NP via intranasal (IN) or intramuscular (IM) routes. Thirty-six days after vaccination, mice were challenged with CoV-OVA and euthanized five days post-challenge. FACS plots (**A**) and graphs (**B**) show flow cytometric analysis of SIINFEKL-specific CD8 T cells in the lungs and quantification of lung viral titers. **C** Graphs show frequencies of granzyme B+, KLRG-1/CX3CR1+ and CD103+ among SIINFEKL- or B8R-specific CD8 T cells following viral challenge. Data are representative of two experiments. Data in each graph indicate mean ± SEM.

(p-STAT3) in SARS-CoV-2-specific CD8 T cells, indicating increased STAT-3 signaling activity (Supplementary Fig. 3). Although we measured total STAT-3 levels in human T cells, previous studies have demonstrated that changes in total STAT-3 expression can influence STAT-3-mediated transcriptional activity and have functional significance[41,42]. Therefore, high levels of STAT-3 might be linked to lower granzyme B expression because STAT-3 negatively regulates the effector transcription program in CD8 T cells[25,26].

IL-6 is one of the potent inducers of STAT-3 and high IL-6 levels is a biomarker of severe COVID-19 in humans[29–34]. However, we find that IL-6 blockade following SARS-CoV-2 infection failed to fully reverse STAT-3 induction or restore granzyme B expression in effector CD8 T cells. This result is not totally unexpected because, (1) therapeutic blockade of IL-6 in COVID-19 patients does not upregulate granzyme B expression in CD8 T cells[51]; (2) there are a number of other molecules including TGF-β that can modulate STAT-3 activity[52]. Nevertheless, these results clearly show that anti-IL-6 therapies might not negatively affect T-cell responses in human COVID-19 patients. What are the possible implications of STAT-3 induction? In addition to suppression of CD8 T-cell effector functions, STAT-3 promotes lung fibrosis[53–57], a sequel to COVID-19 in a cohort of patients. STAT-3 inhibitors are in different phases of clinical trials for cancer therapy [58–60], and STAT-3 targeting might be a potential immunotherapeutic modality to enhance CD8 T-cell immunity and mitigate lung fibrosis in severe COVID-19.

Interestingly, both total STAT-3 expression and phosphorylations of STAT-3 and STAT-5 were reciprocally regulated in SARS-CoV-2- and IAV-specific effector CD8 T cells. A balance between STAT-3 and STAT-5 activities is a defining factor in the development of follicular helper T (T_{FH}) cells versus T_H1 cells; high STAT-3 and STAT-5 activities promote T_{FH} and T_{H1} cell fates, respectively[61,62]. Further, STAT-3 is required for development of the less terminally differentiated T_{CM}s[63] and also predicted to support T_{RM} development and/or maintenance[64]. In essence, STAT-3 opposes terminal differentiation and nurtures less differentiated cell fates such as T_{FH}, T_{CM} and T_{RM}. Therefore, higher STAT-3 phosphorylation in SARS-CoV-2-specific effector CD8 T cells might explain muted terminal differentiation, augmented mucosal imprinting and development of T_{RM}-like effector cells. Diminished STAT-5 phosphorylation in SARS-CoV-2-specific effector CD8 T cells is suggestive of less potent stimulation with γc cytokines such as IL-2/IL-7/IL-15[27,28,65], which in turn might result in exaggerated contraction of effectors, diminished survival and/or defective maintenance of T_{RM}s in lungs of SARS-CoV-2-infected mice.

While we were able to assess both total and phosphorylated STAT-3 levels in our mouse studies, due to limitations in sample availability, we measured only total STAT-3 levels in human T cells. Nevertheless, the observed elevation in total STAT-3 expression suggests altered STAT-3 signaling activity in SARS-CoV-2-infected patients. Future studies involving larger cohorts and direct assessment of STAT-3 activation states would help to further elucidate the role of STAT-3 in human SARS-CoV-2 infections.

To reiterate, the canonical T2 transcription factor GATA-3 was co-induced with STAT-3 in CD4 and CD8 T cells, and a fraction of CD4 T cells in SARS-CoV-2 lungs produced T2 cytokines. There is evidence of similar T2 programming in SARS-CoV-2-infected human patients[66,67]. It is possible that T2 deviation in SARS-CoV-2 lungs is a mechanism that balances the pro-inflammatory T1 responses to limit lung immunopathology. However, it is also conceivable that T2 response along with induction of TGF-β and failure to upregulate inhibitory molecules on T cells might constitute multiple facets of aberrant wound healing or a pro-fibro-inflammatory response, leading to lung fibrosis following recovery from SARS-CoV-2 infection[47,48].

The differentiation pattern of effector CD8 T cells might be epitope-specific, and therefore data from comparison of CD8 T cells in SARS-CoV-2- and IAV- infected K18-ACE2 transgenic mice could be potentially confounding. To address this issue, we engineered a mouse-adapted SARS-CoV-2 strain (CoV-OVA) expressing the SIINFEKL epitope to compare with SIINFEKL-specific CD8 T-cell responses elicited by IAV-OVA. This comparison confirmed the results of disparate effector CD8 T cell differentiation observed in K18-hACE2 transgenic mice, reinforcing the distinction between the CD8 T-cell responses to SARS-CoV-2 and IAV. It is important to note that exposure of K18-hACE2 mice to wild-type SARS-CoV-2 strains results in a more severe infection, often involving the central nervous system and increased morbidity, which are not observed with mouse-adapted strains. Studies using K18-hACE2 mice and wild-type strains of SARS-CoV-2 have shown greater severity in infection outcomes and complications compared to mouse-adapted strains, which provide a more controlled model for studying immune responses[43,68,69]. Notably, despite these differences in pathogenicity, the phenotypes of SARS-CoV-2-elicited CD8 T cells in K18-hACE2 transgenic mice and C57BL/6 mice were largely comparable.

One notable difference between the two mouse models of SARS-CoV-2 infection is highlighted in Fig. 4B; we observed an increase in CD127 expression from day 8 to day 10 in SARS-CoV-2-infected mice, which differs from the pattern seen in our earlier experiments. In Figs. 1 and 2, we utilized K18-hACE2 transgenic mice that are highly susceptible to SARS-CoV-2 infection, leading to severe disease and potentially altering T-cell dynamics. In contrast, the data in Fig. 4 were obtained from wild-type C57BL/6 mice infected with a mouse-adapted SARS-CoV-2 strain. The differences in infection severity between the two models may influence the dynamics of CD127 expression and effector CD8 T-cell differentiation. These findings suggest that the host environment and viral adaptation play significant roles in modulating immune responses during SARS-CoV-2 infection. Further, despite the increased CD103 expression on effector CD8 T cells during the acute phase of SARS-CoV-2 infection, this did not result in higher frequencies of lung TRM cells at memory time points. The significantly lower numbers and frequencies of $CD69^+/CD103^+$ memory CD8 T cells in the lungs and BAL of CoV-OVA-infected mice suggest that SARS-CoV-2 infection may induce aberrant T-cell programming or alter the lung environment in a way that impairs the maintenance or survival of T_{RM} cells. In contrast, IAV infection led to robust establishment of lung TRM cells. This discrepancy indicates that SARS-CoV-2 infection may negatively impact the development and/or long-term persistence of T_{RM} cells.

Using this mouse-adapted SARS-CoV-2 strain expressing the SIINFEKL sequence allowed us to interrogate whether: (1) CD8 T cell responses to a single epitope can provide effective protection against SARS-CoV-2 in lungs without the contribution of CD4 T cells and B cells; (2) secondary effector CD8 T cells differentiate normally from memory CD8 T cells during a breakthrough SARS-CoV-2 infection[70]. Studies have demonstrated that single-epitope-specific CD8 T cells can provide partial protection against SARS-CoV-2. CD8 T-cell responses targeting single epitopes accelerate viral clearance and reduce disease severity[71]. Another study highlighted that T-cell-based vaccines targeting specific epitopes provided protection without the need for antibodies[72]. Additionally, studies identified SARS-CoV-2-specific CD8 T-cell clonotypes and their role in patient protection[73]. Our study further supports these findings, demonstrating that SIINFEKL-specific memory CD8 T cells, induced by vaccination, can effectively differentiate into effector cells and reduce viral loads upon challenge with SARS-CoV-2. Additionally, we show that intranasal and not SC administration of adjuvanted OVA protein resulted in a robust recall response, significantly reducing viral loads and protecting against weight loss following challenge with mouse-adapted CoV-OVA, in a CD8 T cell dependent fashion. This was similarly observed with VV-OVA vaccination, where IN vaccination provided superior protection compared to IM vaccination. These data highlighted the superiority of tissue-resident memory CD8 T cells (induced by IN vaccination) over systemic (induced by SC or IM vaccination) memory CD8 T cells in lung viral control, especially under conditions when there are no contributions from memory CD4 T cells and B cells during the recall response. We have previously shown that mRNA vaccine-induced systemic memory CD8 T cells can provide effective protection against SARS-CoV-2, but this protection is enabled by CD4 T cell-dependent migration of circulatory memory CD8 T cells into the lung parenchyma[14]. It should also be noted that a large fraction of

SIINFEKL-specific CD8 T cells in lungs of CoV-OVA-challenged mice expressed granzyme B, which suggest that SARS-CoV-2 might not impede effector differentiation from memory CD8 T cells during a secondary/recall response, unlike in a primary infection. It is also noteworthy that a majority of SIINFEKL-specific effector CD8 T cells in lungs of CoV-OVA-challenged mice express CD103, and this effect of SARS-CoV-2 to induce CD103 expression is common to both primary and secondary infections.

An interesting finding was that, in the OVA vaccination model, the frequency of SIINFEKL-specific T cells in mucosal tissues appeared reduced, while the $CD103^+$ T_{RM} frequency was increased. The reduced numbers of SIINFEKL-specific T cells in the lungs and BAL despite increased CD103 expression could indicate aberrant T-cell programming influenced by viral factors unique to SARS-CoV-2 infection. These findings suggest that SARS-CoV-2 may differentially affect the maintenance, survival, or localization of tissue-resident memory T cells compared to IAV, possibly through mechanisms that disrupt normal T-cell homeostasis. This discrepancy warrants further investigation to understand the impact of SARS-CoV-2 on mucosal immunity.

It is important to note that our comparisons between SARS-CoV-2 and IAV infections were based on CD8 T-cell responses to single immunodominant epitopes for each virus (K^b/S525 for SARS-CoV-2 and D^b/NP366 for IAV, and K^b/SIINFEKL for SARS-CoV-2 and IAV). Therefore, conclusions regarding the magnitude of the overall T-cell responses are limited to these specific epitopes and may not reflect the full spectrum of T-cell immunity elicited by these infections. Future studies employing more comprehensive methods, such as stimulation with peptide pools and using tetramers spanning multiple viral proteins, would be necessary to fully compare the breadth and magnitude of T-cell responses between SARS-CoV-2 and IAV infections.

In this study, we performed incisive and rigorous assessment of the regulation and programming of the primary T-cell response to SARS-CoV-2 in lungs and investigated the ability of single epitope-specific memory CD8 T cells (induced by mucosal versus parenteral vaccination) to differentiate into effector cells and reduce lung viral load following a breakthrough infection. We find that SARS-CoV-2 and IAV infections drive disparate effector differentiation programs governed by STAT3 and T-bet/EOMES, respectively. The IAV-driven CD8 T cell effector program promotes viral control and protects against immunopathology and fibrosis by balancing strong cytolytic function with the induction of inhibitory receptors such as PD-1, LAG-3 and TIGIT. By contrast, SARS-CoV-2-driven effector program promotes pro-fibrotic inflammation (and accelerated wound healing), evidenced by enhanced STAT3 expression, diminished expression of granzyme B and inhibitory molecules, and elevated CD103 levels. Taken together, data presented in this paper provides fundamental insights into the signaling and transcriptional circuitry underlying the T-cell responses to a primary SARS-CoV-2 infection and identified potential molecular targets such as STAT-3 for immunomodulatory therapies. Finally, our studies utilizing single epitope-specific CD8 T cells highlight their potential in providing targeted protection and reducing viral loads, underscoring the importance of epitope-specific vaccine strategies in combating SARS-CoV-2.

Methods

Human PBMC samples

De-identified peripheral blood mononuclear cell samples collected from healthy volunteers and severely ill COVID-19 patients admitted to the University of Wisconsin hospital were provided by the Translational Science Biocore: Biobank (University of Wisconsin School of Medicine and Public Health). Informed consent was obtained from volunteers who donated experimental samples. All studies were approved by the Institutional Biosafety Committee. While it is known that COVID-19 patients were severely sick, information about the patient demographics, clinical symptoms and therapeutic interventions were not available. All ethical regulations relevant to human research participants were followed.

Experimental animals

All experiments were reviewed and approved by the University of Wisconsin School of Veterinary Medicine Animal Use and Care Committee. 7–12-week-old male C57BL/6J (B6) were purchased from restricted-access specific-pathogen-free (SPF) mouse breeding colonies at the University of Wisconsin-Madison Breeding Core Facility. K18-hACE2 (Stock number: 034860) mice were purchased from Jackson Laboratory or bred in the aforementioned SPF facility. We have complied with all relevant ethical regulations for animal use.

Reagents

Reagents used in these studies are listed in Supplemental Methods and **in** Supplemental Table 1.

Tissue processing and Flow cytometry and ex vivo cytokine analysis

Spleens and lungs were processed into single cell suspensions, and stained for cellular factors as previously described[74] and in Supplemental Methods.

Cells and viruses

Reverse genetics-derived influenza virus strain A/PR/8/34 H1N1 (PR8) was supplied by the Kawaoka lab and propagated in MDCK cells. SARS-CoV-2 USA-WA1/2020 (WA strain) and hCoV-19/South Africa/KRISP-EC-K005321/2020 (SA strain) viruses used in these studies were obtained from BEI resources (NR-52281, NR-55282 respectively) and were cultured as described in Supplemental Methods. The construction of the mouse adapted SARS-CoV-2 virus harboring the SIINFEKL peptide from orf6 was described previously[14].

Vaccination

All vaccinations were administered subcutaneously to the tail base, intramuscularly into the caudal thigh muscle, or intranasally to anesthetized mice in 50 µl saline with 10 µg OVA protein with the following adjuvant combination saline, ADJ (5%) + CpG (5ug). Mice were vaccinated twice at an interval of 3 weeks. Vaccinia virus expressing OVA, or NP[75,76] was administered at a dose of 1×10^7 PFU.

Viral challenge

For SARS-CoV-2 K18-hACE2 mouse studies, sublethal doses were given at 100 PFU, and lethal doses were given at 5×10^4 PFU for both WA and SA strains by the IN route. For PR8 sublethal infection, doses were given at 50 PFU by the IN route. To assess the role of CD8 T cells in protective immunity, mice were administered 200 µg of CD8 T cells (Bio X Cell; Clone 2.43) intravenously and intranasally at days -5. -3, -1 and 1, 3, and 5, relative to challenge as indicated. For IL-6 blocking experiments, K18-hACE2 mice were infected with a sublethal dose of the WA strain of SARS-CoV-2, and intravenously administered with 200 µg of anti-IL-6 (Bio X Cell, Clone: MP5-20F3) at days 0, 2, 4, 6 and 8, relative to viral infection.

Statistical analyses

For all flow cytometry data, identical gates were applied across treatments and samples. Statistical analyses were performed using GraphPad software 9.0 (La Jolla, CA). Planned comparisons were made using a one-way ordinary ANOVA test with multiple comparisons (Fisher's least significant difference test, Fisher's LSD) in group comparisons that did not have significantly different standard deviations as determined by Brown-Forsythe and Bartlett's tests, and if significantly different, multiple comparisons were made using a Brown-Forsythe and Welch test. Two way comparisons were made using an unpaired t test. *, **, ***, and **** indicate significance at $P < 0.05$, 0.005, 0.0005 and 0.00005 respectively. Data in each graph indicate mean ± SEM.

Reporting summary

Further information on research design is available in the Nature Portfolio Reporting Summary linked to this article.

Data availability

Data presented within this study are available within the Supplementary Data file and available from the corresponding author upon request.

Received: 15 July 2024; Accepted: 26 February 2025;
Published online: 08 March 2025

References

1. World Health Organization. data.who.int, WHO Coronavirus (COVID-19) dashboard > Cases. (2023).
2. Centers for Disease Control and Prevention. COVID Data Tracker. Atlanta, GA: U.S. Department of Health and Human Services, CDC. https://www.ebi.ac.uk/ega/ (2024).
3. Muik, A. et al. Neutralization of SARS-CoV-2 Omicron by BNT162b2 mRNA vaccine-elicited human sera. *Science* **375**, 678–680 (2022).
4. Garcia-Beltran, W.F. et al. mRNA-based COVID-19 vaccine boosters induce neutralizing immunity against SARS-CoV-2 Omicron variant. *Cell* **185**, 457–466.e454 (2022).
5. Keeton, R. et al. T cell responses to SARS-CoV-2 spike cross-recognize Omicron. *Nature* **603**, 488–492 (2022).
6. Chen, Z. & John Wherry, E. T cell responses in patients with COVID-19. *Nat. Rev. Immunol.* **20**, 529–536 (2020).
7. Weiskopf, D. et al. Phenotype and kinetics of SARS-CoV-2-specific T cells in COVID-19 patients with acute respiratory distress syndrome. *Sci. Immunol.* **5**, eabd2071 (2020).
8. De Biasi, S. et al. Marked T cell activation, senescence, exhaustion and skewing towards TH17 in patients with COVID-19 pneumonia. *Nat. Commun.* **11**, 3434 (2020).
9. Szabo, P. A. et al. Longitudinal profiling of respiratory and systemic immune responses reveals myeloid cell-driven lung inflammation in severe COVID-19. *Immunity* **54**, 797–814 e796 (2021).
10. Naranbhai, V. et al. T cell reactivity to the SARS-CoV-2 Omicron variant is preserved in most but not all individuals. *Cell* **185**, 1041–1051.e1046 (2022).
11. Neidleman, J. et al. SARS-CoV-2-Specific T cells exhibit phenotypic features of helper function, lack of terminal differentiation, and high proliferation potential. *Cell Rep. Med.* **1**, 100081 (2020).
12. Adamo, S. et al. Signature of long-lived memory CD8(+) T cells in acute SARS-CoV-2 infection. *Nature* **602**, 148–155 (2022).
13. Kingstad-Bakke, B. et al. Vaccine-induced systemic and mucosal T cell immunity to SARS-CoV-2 viral variants. *Proc. Natl Acad. Sci. USA* **119**, e2118312119 (2022).
14. Kingstad-Bakke, B. et al. Airway surveillance and lung viral control by memory T cells induced by COVID-19 mRNA vaccine. *JCI Insight* **8**, e172510 (2023).
15. Jameson, S. C. & Masopust, D. Understanding Subset Diversity in T Cell Memory. *Immunity* **48**, 214–226 (2018).
16. Masopust, D. & Soerens, A. G. Tissue-Resident T cells and other resident leukocytes. *Annu. Rev. Immunol.* **37**, 521–546 (2019).
17. Wang, Z. et al. PD-1(hi) CD8(+) resident memory T cells balance immunity and fibrotic sequelae. *Sci. Immunol.* **4**, eaaw1217 (2019).
18. Dutta, A, et al. LAG-3 expressing antigen-specific CD4+ T cells attenuate lung inflammation during acute influenza virus infection. *J. Immunol.* **196**, 148.141 (2016).
19. Schorer, M. et al. TIGIT limits immune pathology during viral infections. *Nat. Commun.* **11**, 1288 (2020).
20. Evans, R. M. & Lippman, S. M. Shining Light on the COVID-19 Pandemic: a Vitamin D receptor checkpoint in defense of unregulated wound healing. *Cell Metab.* **32**, 704–709 (2020).
21. Ferreira-Gomes, M. et al. SARS-CoV-2 in severe COVID-19 induces a TGF-β-dominated chronic immune response that does not target itself. *Nat. Commun.* **12**, 1961 (2021).
22. Mann, T. H. & Kaech, S. M. Tick-TOX, it's time for T cell exhaustion. *Nat. Immunol.* **20**, 1092–1094 (2019).
23. Chen, Y., Zander, R., Khatun, A., Schauder, D. M. & Cui, W. Transcriptional and epigenetic regulation of effector and memory CD8 T cell differentiation. *Front. Immunol.* **9**, 2826 (2018).
24. Fang, D. & Zhu, J. Dynamic balance between master transcription factors determines the fates and functions of CD4 T cell and innate lymphoid cell subsets. *J. Exp. Med.* **214**, 1861–1876 (2017).
25. Ciucci, T., Vacchio, M. S. & Bosselut, R. A STAT3-dependent transcriptional circuitry inhibits cytotoxic gene expression in T cells. *Proc. Natl Acad. Sci. USA* **114**, 13236–13241 (2017).
26. Zhang, C. et al. STAT3 activation-induced fatty acid oxidation in CD8(+) T effector cells is critical for obesity-promoted breast tumor growth. *Cell Metab.* **31**, 148–161 e145 (2020).
27. Verdeil, G., Lawrence, T., Schmitt-Verhulst, A. M. & Auphan-Anezin, N. Targeting STAT3 and STAT5 in tumor-associated immune cells to improve immunotherapy. *Cancers***11**, 1832 (2019).
28. McGonagle, D., Ramanan, A. V. & Bridgewood, C. Immune cartography of macrophage activation syndrome in the COVID-19 era. *Nat. Rev. Rheumatol.* **17**, 145–157 (2021).
29. Gordon, A. C., Angus, D. C. & Derde, L. P. G. Interleukin-6 Receptor Antagonists in Critically Ill Patients with Covid-19. Reply. *N. Engl. J. Med*. **385**, 1147–1149 (2021).
30. Huang, E. & Jordan, S. C. Tocilizumab for Covid-19 - The Ongoing Search for effective therapies. *N. Engl J. Med.* **383**, 2387–2388 (2020).
31. Hojyo, S. et al. How COVID-19 induces cytokine storm with high mortality. *Inflamm. Regen.* **40**, 37 (2020).
32. Leisman, D. E. et al. Cytokine elevation in severe and critical COVID-19: a rapid systematic review, meta-analysis, and comparison with other inflammatory syndromes. *Lancet Respir. Med.* **8**, 1233–1244 (2020).
33. McGonagle, D., Sharif, K., O'Regan, A. & Bridgewood, C. The Role of Cytokines including Interleukin-6 in COVID-19 induced Pneumonia and Macrophage Activation Syndrome-Like Disease. *Autoimmun. Rev.* **19**, 102537 (2020).
34. Santa Cruz, A. et al. Interleukin-6 is a biomarker for the development of fatal severe acute respiratory syndrome Coronavirus 2 Pneumonia. *Front. Immunol.* **12**, 613422 (2021).
35. Rha, M.-S. et al. PD-1-Expressing SARS-CoV-2-Specific CD8+ T cells are not exhausted, but functional in patients with COVID-19. *Immunity* **54**, 44–52.e43 (2021).
36. Zheng, M. et al. Functional exhaustion of antiviral lymphocytes in COVID-19 patients. *Cell Mol. Immunol.* **17**, 533–535 (2020).
37. Zhou, R. et al. Acute SARS-CoV-2 infection impairs dendritic cell and T cell responses. *Immunity* **53**, 864–877.e865 (2020).
38. Wilk, A. J. et al. A single-cell atlas of the peripheral immune response in patients with severe COVID-19. *Nat. Med.* **26**, 1070–1076 (2020).
39. Codo, A. C. et al. Elevated glucose levels favor SARS-CoV-2 Infection and monocyte response through a HIF-1α/Glycolysis-Dependent Axis. *Cell Metab.* **32**, 498–499 (2020).
40. Rha, M. S. et al. PD-1-Expressing SARS-CoV-2-Specific CD8(+) T cells are not exhausted, but functional in patients with COVID-19. *Immunity* **54**, 44–52.e43 (2021).
41. Aggarwal, B. B. et al. Signal transducer and activator of transcription-3, inflammation, and cancer: how intimate is the relationship? *Ann. N. Y. Acad. Sci.* **1171**, 59–76 (2009).
42. Hossain, D. M. et al. Leukemia cell-targeted STAT3 silencing and TLR9 triggering generate systemic antitumor immunity. *Blood* **123**, 15–25 (2014).
43. Dinnon, K. H. 3rd et al. A mouse-adapted model of SARS-CoV-2 to test COVID-19 countermeasures. *Nature* **586**, 560–566 (2020).
44. Christo, S. N., Park, S. L., Mueller, S. N. & Mackay, L. K. The multifaceted role of tissue-resident memory T Cells. *Annu. Rev. Immunol.* **42**, 317–345 (2024).
45. Zhao, Y. et al. Clonal expansion and activation of tissue-resident memory-like Th17 cells expressing GM-CSF in the lungs of severe COVID-19 patients. *Sci. Immunol.* **6**, eabf6692 (2021).

46. Kusnadi, A. et al. Severely ill COVID-19 patients display impaired exhaustion features in SARS-CoV-2-reactive CD8+ T cells. *Sci. Immunol.* **6**, eabe4782 (2021).
47. Melms, J. C. et al. A molecular single-cell lung atlas of lethal COVID-19. *Nature* **595**, 114–119 (2021).
48. Delorey, T. M. et al. COVID-19 tissue atlases reveal SARS-CoV-2 pathology and cellular targets. *Nature* **595**, 107–113 (2021).
49. Zammit, D. J., Turner, D. L., Klonowski, K. D., Lefrançois, L. & Cauley, L. S. Residual antigen presentation after influenza virus infection affects CD8 T cell activation and migration. *Immunity* **24**, 439–449 (2006).
50. Kim, T. S., Hufford, M. M., Sun, J., Fu, Y. X. & Braciale, T. J. Antigen persistence and the control of local T cell memory by migrant respiratory dendritic cells after acute virus infection. *J. Exp. Med.* **207**, 1161–1172 (2010).
51. Mazzoni, A. et al. Impaired immune cell cytotoxicity in severe COVID-19 is IL-6 dependent. *J. Clin. Investig.* **130**, 4694–4703 (2020).
52. Rébé, C., Végran, F., Berger, H. & Ghiringhelli, F. STAT3 activation: a key factor in tumor immunoescape. *Jakstat* **2**, e23010 (2013).
53. Chakraborty, D. et al. Activation of STAT3 integrates common profibrotic pathways to promote fibroblast activation and tissue fibrosis. *Nat. Commun.* **8**, 1130 (2017).
54. Dees, C. et al. TGF-β–induced epigenetic deregulation of SOCS3 facilitates STAT3 signaling to promote fibrosis. *J. Clin. Investig.* **130**, 2347–2363 (2020).
55. Simonian, P. L. et al. Th17-Polarized immune response in a murine model of hypersensitivity pneumonitis and lung fibrosis. *J. Immunol.* **182**, 657–665 (2009).
56. Le, T.-T. T. et al. Blockade of IL-6 Trans Signaling Attenuates Pulmonary Fibrosis. *J. Immunol.* **193**, 3755–3768 (2014).
57. Fielding, C. A. et al. Interleukin-6 signaling drives fibrosis in unresolved inflammation. *Immunity* **40**, 40–50 (2014).
58. Jonker, D. J. et al. Napabucasin versus placebo in refractory advanced colorectal cancer: a randomised phase 3 trial. *Lancet Gastroenterol. Hepatol.* **3**, 263–270 (2018).
59. Kawazoe, A. et al. Multicenter Phase I/II Trial of Napabucasin and Pembrolizumab in Patients with Metastatic Colorectal Cancer (EPOC1503/SCOOP Trial). *Clin. Cancer Res.* **26**, 5887–5894 (2020).
60. Zou, S. et al. Targeting STAT3 in cancer immunotherapy. *Mol. Cancer* **19**, 145 (2020).
61. Oestreich, K. J. & Weinmann, A. S. T-bet employs diverse regulatory mechanisms to repress transcription. *Trends Immunol.* **33**, 78–83 (2012).
62. Ray, J. P. et al. Transcription factor STAT3 and type I interferons are corepressive insulators for differentiation of follicular helper and T helper 1 cells. *Immunity* **40**, 367–377 (2014).
63. Siegel, A. M. et al. A critical role for STAT3 transcription factor signaling in the development and maintenance of human T cell memory. *Immunity* **35**, 806–818 (2011).
64. Milner, J. J. & Goldrath, A. W. Transcriptional programming of tissue-resident memory CD8(+) T cells. *Curr. Opin. Immunol.* **51**, 162–169 (2018).
65. Leonard, W. J., Lin, J. X. & O'Shea, J. J. The gammac family of cytokines: basic biology to therapeutic ramifications. *Immunity* **50**, 832–850 (2019).
66. Gil-Etayo, F. J. et al. T-Helper cell subset response is a determining factor in COVID-19 progression. *Front. Cell Infect. Microbiol.* **11**, 624483 (2021).
67. Roncati, L., Nasillo, V., Lusenti, B. & Riva, G. Signals of Th2 immune response from COVID-19 patients requiring intensive care. *Ann. Hematol.* **99**, 1419–1420 (2020).
68. Golden, J. W. et al. Human angiotensin-converting enzyme 2 transgenic mice infected with SARS-CoV-2 develop severe and fatal respiratory disease. *JCI Insight* **5**, e142032 (2020).
69. Winkler, E. S. et al. SARS-CoV-2 infection of human ACE2-transgenic mice causes severe lung inflammation and impaired function. *Nat. Immunol.* **21**, 1327–1335 (2020).
70. Tada, T., Peng, J. Y., Dcosta, B. M. & Landau, N. R. Single-epitope T cell-based vaccine protects against SARS-CoV-2 infection in a preclinical animal model. *JCI Insight* **8**, e167306 (2023).
71. van Bergen, J. et al. Multiantigen pan-sarbecovirus DNA vaccines generate protective T cell immune responses. *JCI Insight* **8**, e172488 (2023).
72. Shi, J. et al. A T cell-based SARS-CoV-2 spike protein vaccine provides protection without antibodies. *JCI Insight* **9**, e155789 (2024).
73. Xie, J. & Heath, J. 1539 SARS-CoV-2 genome-wide single-chain-trimer peptide-MHCs reveal CD8+ T cell landscape in COVID-19 patients and distinct TCR repertoire dynamics. *J. ImmunoTherapy Cancer* **11**, A1764–A1764 (2023).
74. Marinaik, C. B. et al. Programming multifaceted pulmonary T cell immunity by combination adjuvants. *Cell Rep. Med.* **1**, 100095 (2020).
75. Whitton, J. L., Southern, P. J. & Oldstone, M. B. Analyses of the cytotoxic T lymphocyte responses to glycoprotein and nucleoprotein components of lymphocytic choriomeningitis virus. *Virology* **162**, 321–327 (1988).
76. Restifo, N. P. et al. Antigen processing in vivo and the elicitation of primary CTL responses. *J. Immunol.* **154**, 4414–4422 (1995).

Acknowledgements

We thank Daisy Gates for expert technical assistance for K18-hACE2 mice genotyping and assisting with tissue processing. Thanks to Drs. Kawaoka and Halfmann for providing K18-hACE2 mice. We thank the Emory NIH Tetramer Core Facility for providing MHC-I tetramers. We also thank the efforts of the veterinary and animal care staff at UW-Madison. This work was supported by PHS grant U01 AI124299, R21 AI149793-01A1 and John E. Butler professorship to M. Suresh. Woojong Lee was supported by a pre-doctoral fellowship from the American Heart Association (18PRE34080150).

Author contributions

B.K.B., W.L., and M.S. designed, performed and analyzed experiments, and provided conceptual input for the manuscript. T.C. and H.P. performed experiments and analyzed data. B.Y. and R.B. generated recombinant the recombinant SARS-CoV-2 virus. J.S. provided critical resources and conceptual input for designing experiments. B.K.B. and M.S. wrote the manuscript, which was proofread by all authors. The authors declare no competing interests.

Competing interests

The authors declare no competing interests.

Additional information

Supplementary information The online version contains supplementary material available at https://doi.org/10.1038/s42003-025-07820-7.

Correspondence and requests for materials should be addressed to M. Suresh.

Peer review information *Communications Biology* thanks Sarah Adamo and the other, anonymous, reviewer(s) for their contribution to the peer review of this work. Primary Handling Editor: Dario Ummarino.